

# Mitochondrial fission factor drives an actionable metabolic vulnerability in multiple myeloma

Maria Eugenia Gallo Cantafio,<sup>1</sup> Ilenia Valentino,<sup>1\*</sup> Roberta Torcasio,<sup>1-3\*</sup> Ludovica Ganino,<sup>1</sup> Claudia Veneziano,<sup>1</sup> Pierpaolo Murfone,<sup>1</sup> Maria Mesuraca,<sup>1</sup> Ida Perrotta,<sup>4</sup> Federico Tallarigo,<sup>5</sup> Valter Agosti,<sup>1</sup> Carmela De Marco,<sup>1</sup> Teresa Pasqua,<sup>6</sup> Cesarina Giallongo,<sup>7</sup> Anna Rita Cappello,<sup>8</sup> Marco Fiorillo,<sup>8</sup> Massimo Gentile,<sup>8,9</sup> Daniele Tibullo,<sup>10</sup> Giuseppe Viglietto,<sup>1</sup> Antonino Neri<sup>11</sup> and Nicola Amodio<sup>1</sup>


<sup>1</sup>Department of Experimental and Clinical Medicine, Magna Graecia University of Catanzaro, Catanzaro, Italy; <sup>2</sup>Department of Biology, Ecology and Earth Sciences, University of Calabria, Rende, Italy; <sup>3</sup>Department of Medical Oncology, Dana-Farber Cancer Institute, Harvard Medical School, Boston, MA, USA; <sup>4</sup>Department of Biology, Ecology and Earth Sciences, Center for Microscopy and Microanalysis, University of Calabria, Rende, Italy; <sup>5</sup>COR Calabria, Public Health Unit, Crotone, Italy; <sup>6</sup>Department of Health Science, Magna Graecia University of Catanzaro, Catanzaro, Italy; <sup>7</sup>Department of Medical, Surgical Sciences and Advanced Technologies “G.F. Ingrassia” University of Catania, Catania, Italy; <sup>8</sup>Department of Pharmacy, Health and Nutritional Sciences, University of Calabria, Rende, Italy; <sup>9</sup>Department of Onco-hematology, Hematology Unit, Azienda Ospedaliera Annunziata, Cosenza, Italy; <sup>10</sup>Department of Biomedical and Biotechnological Sciences, University of Catania, Catania, Italy and <sup>11</sup>Scientific Directorate, Azienda USL-IRCCS di Reggio Emilia, Reggio Emilia, Italy

*\*IV and RT contributed equally.*

**Correspondence:** N. Amodio  
[amodio@unicz.it](mailto:amodio@unicz.it)

**Received:** February 14, 2025.  
**Accepted:** May 9, 2025.  
**Early view:** May 22, 2025.

**<https://doi.org/10.3324/haematol.2025.287526>**

©2025 Ferrata Storti Foundation  
Published under a CC BY-NC license 

# Mitochondrial Fission Factor drives an actionable metabolic vulnerability in multiple myeloma

Maria Eugenia Gallo Cantafio<sup>1</sup>, Ilenia Valentino<sup>1†</sup>, Roberta Torcasio<sup>1,2,3†</sup>, Ludovica Ganino<sup>1</sup>, Claudia Veneziano<sup>1</sup>, Pierpaolo Murfone<sup>1</sup>, Maria Mesuraca<sup>1</sup>, Ida Perrotta<sup>4</sup>, Federico Tallarigo<sup>5</sup>, Valter Agosti<sup>1</sup>, Carmela De Marco<sup>1</sup>, Teresa Pasqua<sup>6</sup>, Cesarina Giallongo<sup>7</sup>, Anna Rita Cappello<sup>8</sup>, Marco Fiorillo<sup>8</sup>, Massimo Gentile<sup>8,9</sup>, Daniele Tibullo<sup>10</sup>, Giuseppe Viglietto<sup>1</sup>, Antonino Neri<sup>11</sup>, and Nicola Amodio<sup>1\*</sup>

<sup>1</sup>Department of Experimental and Clinical Medicine, Magna Graecia University of Catanzaro, Viale Europa, Campus Germaneto, 88100 Catanzaro, Italy

<sup>2</sup>Department of Biology, Ecology and Earth Sciences, University of Calabria, 87036 Rende, Italy

<sup>3</sup>Department of Medical Oncology, Dana-Farber Cancer Institute, Harvard Medical School, Boston, Massachusetts

<sup>4</sup>Department of Biology, Ecology and Earth Sciences, Centre for Microscopy and Microanalysis, University of Calabria, 87036 Rende, Italy

<sup>5</sup>COR Calabria, Public Health Unit, 88900 Crotone, Italy

<sup>6</sup>Department of Health Science, University Magna Graecia of Catanzaro, 88100, Catanzaro, Italy

<sup>7</sup>Department of Medical, Surgical Sciences and Advanced Technologies "G.F. Ingrassia", University of Catania, 95123 Catania, Italy

<sup>8</sup>Department of Pharmacy, Health and Nutritional Sciences, University of Calabria, 87036 Rende, Italy

<sup>9</sup>Department of Onco-hematology, Hematology Unit, Azienda Ospedaliera Annunziata, Cosenza, Italy

<sup>10</sup>Department of Biomedical and Biotechnological Sciences, University of Catania, 95123, Catania, Italy

<sup>11</sup>Scientific Directorate, Azienda USL-IRCCS di Reggio Emilia, 42123 Reggio Emilia, Italy

<sup>†</sup>These authors equally contributed to the study

**\*Corresponding author:** Prof. Nicola Amodio; e-mail: amodio@unicz.it

## **Supplementary methods**

### **Cell culture, drugs and oligonucleotides**

Human MM cell lines were cultured in RPMI-1640 medium supplemented with 10% heat inactivated fetal bovine serum (FBS) (Gibco®, Life Technologies, Carlsbad, CA), 100 U/mL Penicillin and 100 µg/mL Streptomycin (P/S) (Gibco®, Life Technologies, Carlsbad, CA), and maintained at 37°C in a 5% CO<sub>2</sub> atmosphere. All the cell lines were periodically tested for mycoplasma contamination. AMO and AMO-BZB cells were kindly provided by Dr. Driessen (University of Tübingen, Germany). NCI-H929 was purchased from DSMZ (Braunschweig, Germany), which certified authentication performed by short tandem repeat DNA typing. NCI-H929-BZB and NCI-H929-CFZ cells were selected for bortezomib (BZB) and carfilzomib (CFZ) resistance by exposure to progressively higher concentrations of BZB or CFZ. The HS5 cell line was purchased from the American Type Culture Collection (Rockville, MD, USA). Peripheral blood mononuclear cells (PBMCs) were isolated by Ficoll-hypaque (Lonza Group, Basel, Switzerland) from healthy donors, following informed consent and Institutional Review Board (University of Catanzaro, Catanzaro, Italy) approval (institutional approval: n.266/2021). PBMCs were cultured in RPMI-1640 medium (Gibco®, Life Technologies) supplemented with 10% fetal bovine serum (Lonza Group Ltd.) and 1% penicillin/streptomycin (Gibco®, Life Technologies).

Bortezomib (#S1013), IACS-010759 (#S8731), Syrosingopine (Su3118; #S9907), and AZD3965 (#S7339) DMSO solutions were purchased from Selleck Chemicals LLC (Munich, Germany). L-Lactate (#867-56-1), Mdivi-1 (#338967-87-6), and Oroboros reagents, including Oligomycin (#O4876), FCCP (#C2920), and Antimycin A (#A8674), were purchased from Sigma Aldrich (USA). LNA-gapmeR antisense oligonucleotides (ASOs) anti-MFF were purchased from Exiqon (Vedbaek, Rudersdal, Denmark); the sequence are: TACGAGTAGAAGACTG (g\_01); TGAAGTGTGCGATGCAA (g\_02); ACTTTACACAACAATT (g\_03); AACATGCAAAGGGAGA (g\_04); ACTGAGTAAAAACGTA (g\_05); GCTTCTGTGCTTCATA (g\_06); as control, a LNA-gapmeR ASO negative control AACACGTCTATACGC (g\_NC) was used. Silencer® Select siRNA for MFF (siMFF, cat #4392420, ID: s533050, ID: s533051), or control (siNC, cat #AM4611) were purchased from Thermo Fisher Scientific (Waltham, MA, USA).

### **Transmission Electron Microscopy (TEM)**

Samples were processed for ultrastructural TEM analysis according to standard protocols.<sup>1,2</sup> Cell pellets were fixed in 3% glutaraldehyde (Merck Sigma-Aldrich) in 0.1 M

phosphate buffer at pH 7.4 (Clinical Sciences) for 2 h at 4 °C. After 2 h, three washes were carried out in phosphate buffer at 4 °C to eliminate any residual fixative. A post-fixation in 1% osmium tetroxide in phosphate buffer (0.1 M, pH 7.4) was then performed for 2 h at 4°C to preserve the lipid structures. Samples were washed 3 times in a phosphate buffer, subjected to gradual dehydration using increasing concentrations of acetone, and embedded with epoxy resin (Epon). Ultrathin sections (60–90 nm) were obtained using an RMC PowerTome series ultramicrotome with a Diatome diamond knife, collected on 300 mesh copper grids, and observed with a Jeol JEM-1400 Plus transmission electron microscope operating at 80 kV. Morphometric analyses of TEM images were performed with ImageJ (version 1.52i, National Institutes of Health, Bethesda, MD, USA) on a sample of 15 systematically, uniformly, and randomly selected images for each group. Data (presented as mean  $\pm$  S.E.) were analyzed by the one-way analysis of variance (ANOVA) and Tukey's test.

### **Multi-Omics Data in CoMMpass Study**

Multi-omics data about bone marrow MM samples at baseline (BM\_1) were publicly accessible from MMRF CoMMpass Study (<https://research.themmr.org/>) including more than 1000 MM patients from several worldwide sites and retrieved from the Interim Analysis 15a (MMRF\_CoMMpass\_IA15a, accessed on 16 October 2020). Transcript per Million (TPM) reads values of the MFF transcript were retrieved using Salmon gene expression quantification data (MMRF\_CoMMpass\_IA15a\_E74GTF\_Salmon\_V7.2\_Filtered\_Gene\_TPM) in 774 BM\_1 MM patients. Non-synonymous (NS) somatic mutation variants and counts data were obtained from whole exome sequencing (WES) analyses, main IgH translocations were inferred from RNA-seq spike expression estimates of known target genes and Copy Number Alteration (CNA) data were retrieved by means of Next generation Sequencing (NGS)-based fluorescence in situ hybridization (FISH)<sup>3</sup> in 660 MM cases for which all data were available. The presence of a specific CNA was considered when occurring in at least one of the investigated cytoband at a 20 percent cut-off for each considered chromosomal aberration, as previously reported.<sup>4</sup>

### **RNA-sequencing, Differential Gene Expression (DEG) and Pathway Analyses**

RNA was quantified using a Qubit™ RNA HS Assay kit (Thermo Fisher Scientific, MA, USA) and integrity determined on the Agilent 2200 System by the Agilent High Sensitivity

RNA Assay (Agilent Technologies, Santa Clara, CA). Library preparation was manually performed using the Ion AmpliSeq™ Transcriptome Human Gene Expression Core Panel (Thermo Fisher Scientific), according to the Ion AmpliSeq Library Kit Plus (Thermo Fisher Scientific). Briefly, 10 ng of RNA was reverse transcribed with SuperScript™ Vilo™ cDNA Synthesis Kit (Thermo Fisher Scientific). The resulting cDNA was amplified to prepare barcoded libraries using the Ion Xpress™ Barcode Adapters (Thermo Fisher Scientific), according to the manufacturer's instructions. Barcoded libraries were combined to a final concentration of 50 pM and loaded on Ion 540™ Chips, using the Ion 540™ Kit-Chief (Thermo Fisher Scientific). Sequencing was performed on the Ion GeneStudio S5™ System with Torrent Suite™ Software v5.14.0 (Thermo Fisher Scientific).

Differential gene expression (DEG) was analyzed using Transcriptome Analysis Console Software v4.0.3.14 (Thermo Fisher Scientific). The analysis was performed with a fold change (FC) greater than 2 or less than -2, p-value<0.05, false discovery rate (FDR)<0.05. Gene set enrichment analysis (GSEA) v4.3.2 (<https://www.gsea-msigdb.org/gsea/msigdb>) was applied on commonly deregulated between shMFF and OE MFF transcript profiles to identify significantly enriched gene sets Hallmark signatures database. False discovery rate (FDR) less than 25% after 1000 random permutations was set as the cutoff criterion. To define glycolysis and oxidative phosphorylation signatures, related genes were downloaded from GSEA as previously described.<sup>5</sup>

### **Virus generation and transduction of MM cells**

H929 MM cells stably overexpressing the MFF gene were generated using the lentiviral pLenti.PGK.blast-Flag-MFF-WT vector for Homo sapiens MFF (cat#74379, Addgene), as previously described.<sup>6</sup> Lentiviral particles were produced by co-transfecting HEK293T cells with 10 µg of plasmid construct and packaging vectors (10 µg of p-CMV-VSVG and 4 µg of Delta 8.9 plasmids). Empty control vector EX-NEG-Lv181 lentivirus (Genecopoeia) was used as a control. Supernatants containing lentiviral particles were harvested after 48 hours and sterile 0.45 µm filtered. MM cells were spinoculated for 1 hour with media containing lentiviral particles, in the presence of 8 µg/mL polybrene, as previously reported<sup>7</sup>; the selection of stable clones was carried out using blasticidin (4 µg/ml).

Custom cloning of shRNAs targeting MFF (shRNA MISSION®, TRCN0000343572; TRCN0000343573; TRCN0000343574) or the scramble control (Mission shRNA set, Sigma Aldrich-Merk) were purchased from Merck Life Science (Italy). Lentiviral particles production and transduction were performed according to the above-mentioned protocol;

the selection of stable clones was carried out using puromycin (0.5 µg/ml). The knock-down (KD) or overexpression (OE) efficiency was validated by detecting MFF mRNA and/or protein levels by qRT-PCR and western blotting, respectively.

### **Transient transfection of MM cells**

MM cells were transfected by electroporation using Neon Transfection System (Invitrogen, CA, USA), according to user guidelines (electroporation protocol: 2 pulses at 1150 v, 30 ms) and previously established protocols.<sup>8</sup> LNA gapmeRs or siRNAs were used at 100 nM final concentration. The transfection efficiency was evaluated by western blotting analysis of MFF protein levels.

### **Cell viability and clonogenicity assays**

Cell Titer Glo (CTG) assay kit (Promega, Madison, WI, USA) was used to evaluate cell viability, according to manufacturer's instructions. Briefly, MM cells were seeded in 24-well plates after electroporation and the effects of g\_05 and g\_06 as well as siRNAs on cell viability were evaluated at 48h. Luminescence was recorded using a GloMax-multi detection system (Promega, Madison, WI, USA).

For combination experiments, MM cells were seeded in 24-well plates and treated with different concentrations of Mdivi-1 or Bortezomib, with Syrosingopine and AZD3965. After 48h, MM cells were collected and luminescence was recorded using a GloMax multi-detection system (Promega, Madison, WI, USA).

Drug combination studies and their synergy quantification followed the Chou-Talalay method<sup>9</sup>, a mathematical method commonly used to quantify drug interactions. Combination indexes (CI) were calculated by CalcuSyn software (BIOSOFT, Cambridge, UK). CI<1 synergic; CI=1 additive effect; CI>1 antagonism.

Cell proliferation of shMFF MM cells was assessed using a trypan blue exclusion assay. Briefly, MM cells stably silenced for MFF were plated in 6-well plates, and viable cells were counted on days 0, 6, and 9 using the trypan blue reagent.

For co-culture experiments, AMO-BZB cells were seeded onto HS5 cells at a 1:2 ratio in 24-well plates and co-cultured with physical separation using Transwell cell culture permeable supports (Corning, USA). After 48 hours, a CTG assay was used to evaluate MM cell viability, and the final luminescence was recorded using the GloMax plate reader.

For the colony-forming assay, MM cells were plated in triplicate in 24-well plates, in 1mL of mixture containing 1.1% methylcellulose (MethoCult STEMCELL) and RPMI-1640

supplemented with 10% FBS. The cell suspension was then allowed to grow in a humidified incubator at 37°C for 10 days. Following incubation, colonies were fixed with methanol, stained with crystal violet solution (0.04%), and counted under a light microscope (Leica DM IL LED).

### **Cell cycle analysis**

The cell cycle distribution was analyzed using flow cytometry following propidium iodide (PI) staining (Sigma Aldrich). Briefly, cells were harvested at specific time points, washed with cold PBS, and fixed in 70% ethanol at -20°C overnight. After fixation, cells were washed with PBS and incubated with the staining solution containing RNase A (for RNA removal) and propidium iodide (PI; 50 µg/mL) at room temperature in the dark for 60 minutes. Flow cytometry analysis was performed using the FACS Fortessa X-20 instrument (BD Biosciences, San Jose, CA, USA), and the DNA content was measured to determine the distribution of cells in the G0/G1, S, and G2/M phases. The data were analyzed using FlowJo software version 10, and the percentage of cells in each cell cycle phase was determined based on DNA content analysis.

### **Measurements of mitochondrial ROS and mitochondrial membrane potential**

Mitochondrial ROS production was measured using Mito-SOX™ Red mitochondrial superoxide indicator (Thermo Fisher Scientific) whereas mitochondrial membrane potential was evaluated using TMRM probe (Thermo Fisher Scientific), according to manufacturer's instructions. After 48h of electroporation with g\_06 or g\_NC gapmers, AMO-BZB cells were stained with 5 µM MitoSOX Red or 100 nM TMRM and incubated for 30 minutes at 37°C in the dark. Stained cells were acquired by using FACS Fortessa X-20 (BD Biosciences). All experiments were performed in triplicate and for each sample at least 1x10<sup>4</sup> events were acquired. FlowJo software version 10 was used for data analysis.

### **Measurement of OCR and ECAR by Seahorse Analyzer**

MM cell lines were seeded in a Seahorse XFe96 Cell Culture Microplate (Agilent) at a density of 3x10<sup>4</sup> cells per well (10 technical replicates) in 180 µl of XF RPMI medium supplemented with 25 mM glucose and 2 mM glutaMAX. The oxygen consumption rate (OCR) and extracellular acidification rate (ECAR) were quantified using the Seahorse Extracellular Flux Analyzer (XFe96, Agilent Technologies). Measurement time was 30 seconds following 3 minutes mixture and 30 seconds waiting time. First three cycles were

used for basal respiration quantification. The sequential addition of the ATP synthase inhibitor oligomycin, the uncoupler FCCP, and the respiratory complex III inhibitor antimycin A, was carried out and basal respiration, ATP production and maximal respiration were calculated following the manufacturer's instructions. Basal respiration is calculated as the last rate measurement before oligomycin injection – non-mitochondrial respiration rate. Maximal respiration is calculated as the maximum rate measurement after FCCP injection – non-mitochondrial respiration rate. Protein quantification was used to normalize the results.

### **Oroboros O2k-High resolution Respirometer**

The oxygen consumption was analyzed in 2 mL chambers at 37°C using the Oroboros Oxygraph-2k high resolution respirometer (Oroboros Instrument, Innsbruck, Austria), following the procedures of the SUIT protocol D009. MM cells silenced or overexpressing MFF cultured in basal conditions or treated with 10 mM L-Lactate or vehicle were subjected to respirometry analysis. After instrumental calibration, MM cells were collected and loaded in the O2k-closed chambers at a density of  $1 \times 10^6$  per mL, for a total of 2 mL of complete medium per chamber, by maintaining cell suspension continuously mixed. First, the basal respiration was recorded as routine respiration (before adding reagents). Then, variations of respirations were measured after sequential addition of oligomycin, FCCP, and antimycin A, evaluating the LEAK state, the maximal respiration and the residual oxygen consumption, respectively. Reagents were added into the closed chamber by Hamilton syringes (Oroboros Instruments, Innsbruck, Austria). Data acquisition and analysis were performed using DatLab software (Oroboros Instrument, Innsbruck, Austria). Measurements were normalized for the cell count and protein quantification.  $O_2$  flow is expressed per cell [ $\text{amol} \cdot \text{s}^{-1} \cdot \text{x}^{-1}$ ] equivalent to [ $\text{pmol} \cdot \text{s}^{-1} \cdot (10^6 \text{ cells})^{-1}$ ].

### **Intracellular Lactate measurement**

The intracellular concentration of L-Lactate in MM cells was determined by using the Lactate-Glo Assay purchased from Promega (Madison, WI, USA), according to manufacturer's instructions. Briefly, 50  $\mu\text{L}$  of samples were transferred in 96 well plates and added with the same volume of Lactate Detection Reagent (ratio 1:1). After 1h of incubation, luminescence was measured by using GloMax plate reader (Promega, Madison, WI, USA). At least three replicates were included for each measurement.



### **Apoptosis detection**

Apoptosis was evaluated by Annexin V/7-Aminoactinomycin D (7-AAD) flow cytometry assay (BD biosciences). MM cells were stained in a 5 mL polystyrene tube, following the protocol of the PE/Annexin V Apoptosis Detection Kit (Thermo Fisher Scientific, Waltham, MA, USA). After the appropriate treatments, MM cells were collected, washed with PBS 1X, and exposed to Annexin V-PE and 7-AAD probes for 15 min at room temperature. Samples were run on a FACS Fortessa X-20 instrument (BD Biosciences, San Jose, CA, USA); data were analyzed using the FlowJo software version 10 and presented as histogram bars, indicating the percentage of early and late apoptotic cells.

### **Western blotting (WB) and immunoprecipitation assay (IP)**

Total protein extracts were prepared using NP40 Cell Lysis Buffer supplemented with Halt Protease Inhibitor Single-Use Cocktail (Thermo Fisher Scientific, Waltham, MA, USA). Protein samples (30 µg) were run in 10% SDS-PAGE and then transferred to nitrocellulose membranes using the Trans-Blot Turbo Transfer System (Bio-Rad Laboratories, Hercules, CA, USA); membranes were next subjected to immunoblotting using the following primary antibodies: MFF (#84580S), DRP1 (#14647S), NDUFS1 (#70264), NDUFAB1 (#71814), UQCRC1 (#95231), COX1 (#55159), and COX IV (#4850); LDHB (#56298); GAPDH (#5174) was used as loading control. All antibodies were purchased from Cell Signaling Technology (MA, USA). The  $\gamma$ -tubulin (T6557) antibody was used as loading control and was purchased from Sigma-Aldrich (St. Louis, Missouri, USA). The Pan-KLA (STJ11101522) antibody was purchased from St John's Laboratory (London, UK). Chemiluminescence was detected using Clarity Western ECL Substrate (Biorad Laboratories, USA). Signal intensity was quantified by UVITEC Imaging Systems (Cleaver Scientific, UK).

For IP experiments, 1.5 milligrams of cell lysates were used to isolate Drp1 or MFF-interacting proteins employing Protein A/G-Plus Agarose (sc-2003; Santa Cruz Biotechnology, TX, USA) to capture the protein complexes. First, Protein A/G-Plus agarose beads were washed three times with NP40 buffer before being added to a mixture containing cell lysate, and either Drp1 antibody, MFF antibody, or an isotype Ig control. The mixture was then incubated overnight at 4°C with gentle agitation; next, IP products were washed three times with NP40 buffer, proteins eluted from the beads using a denaturing buffer, and separated by WB.

### **Reverse transcription and quantitative real-time amplification (qRT-PCR)**

RNA extraction, reverse transcription (RT), and quantitative real-time amplification (qRT-PCR) were carried out following previously described methods.<sup>8</sup> Total RNA was extracted from MM cells using TRIzol Reagent (Thermo Fisher Scientific, Waltham, MA, USA) according to the manufacturer's protocol; the integrity and purity of the isolated total RNA were assessed using a Nanodrop Spectrophotometer nd-2000 (Thermo Fisher Scientific, Waltham, MA, USA). To quantify the expression levels of MFF (Hs00697394\_g1) gene, a single-tube TaqMan mRNA assay (Applied Biosystems, Thermo Fisher Scientific, USA) was employed, following manufacturer's instructions. Normalization was performed using human GAPDH (Hs03929097\_g1). To quantify the expression levels of ALDOC, HK2, ENO2, PDK4, SLC2A1, MCT1, MCT4, and LDHB, Sybr Green solution, purchased by Applied Biosystems, was employed following manufacturer's instructions. Comparative qRT-PCR was performed in triplicate, including no-template controls, by using QuantStudio 12K Flex reader (Thermo Fisher Scientific, Waltham, MA, USA). Relative expression was calculated using the comparative threshold (Ct) method. Normalization was performed using human  $\beta$ -Actin.

The sequence of primers, purchased by Eurofins, was the following:

ALDO fwd (5'- CATTCTGGCTGCGGATGAGTC -3')

ALDO rev (5'- CACACGGTCATCAGCACTGAAC -3')

ENO2 fwd (5'- CTCTGTGGTGGAGCAAGAGA -3')

ENO2 rev (5'- ATTGATCACGTTGAAGGCCG -3')

HK2 fwd (5'- TCCCAACTCTGCGCCGTCG -3')

HK2 rev (5'- AGGCGCATGTGGTAGAGATACTG -3')

PDK4 fwd (5'- AGGTGGAGCATTCTCGCGCTA -3')

PDK4 rev (5'- GAATGTTGGCGAGTCTCACAGG -3')

SLC2A1 fwd (5'- TTGCAGGCTTCTCCAACTGGAC -3')

SLC2A1 rev (5'- CAGAACCAGGAGCACAGTGAAG -3')

MCT1 fwd (5'- TTGTTGGTGGCTGCTTGTCAGG -3')

MCT1 rev (5'- CAATCATGGTCAGAGCTGGATTCAAG -3')

MCT4 fwd (5'- GCCATCTTTGCTGGTGGTTACC -3')

MCT4 rev (5'- TGGTCCAGAAAGGACAGCCATC -3')

LDHB-fwd (5'- GGACAAGTTGGTATGGCGTGTG -3')

LDHB-rev (5'- AAGCTCCCATGCTGCAGATCCA -3')

β-Actin fwd (5'- CAAGGCCAACCGCGAGAAGATGAC -3')

β-Actin rev (5'- GCCAGAGGCGTACAGGGATAGCACA -3')

### ***In vivo study***

Male SCID.NOD mice (6- to 8-weeks old; Envigo, Indianapolis) were housed and monitored in our Animal Research Facility. All the experimental procedures were carried out at University Magna Graecia of Catanzaro under the Italian MOH authorization n.887/2021-PR, and performed according to protocols approved by the National Directorate of Veterinary Services (Italy) and the Institutional Ethical Committee (Magna Graecia University of Catanzaro). According to institutional guidelines, mice were sacrificed when tumors reached 2 cm in diameter or in the case of paralysis or significant compromise in their quality of life, in order to mitigate unnecessary suffering. Mice were subcutaneously inoculated with  $5.0 \times 10^6$  AMO-BZB cells stably transduced with an MFF-targeting shRNA or a scrambled control (SCR). When tumors became palpable (100–200 mm<sup>3</sup>; ≈3 weeks after injection; n= 5 mice/group), tumor volume was measured by an electronic Caliper using the following formula:  $V = (a^2 \times b)/2$ , where  $a$  is the width and  $b$  is the length of the tumor.

### **Immunohistochemistry (IHC)**

Retrieved tumors from treated mice were immersed in 4% buffered formaldehyde, and 24 h later washed, dehydrated, and embedded in paraffin. Hematoxylin–eosin (H&E) staining was performed on 4μm sections mounted on polylysine slides. Tissues sections were observed under the OLYMPUS BX51 optical microscope (Olympus Corporation, Tokyo, Japan). For IHC staining, tumor slices (2 μm size) were deparaffinized and pre-treated with the Epitope Retrieval Solution 2 (EDTA-buffer, pH 8.8) at 98 °C for 20 min. After washing steps, peroxidase blocking was carried out for 10 min using the Bond Polymer. All procedures were performed using the Benchmark XT-Automated Immunohistochemistry instrument (Ventana Medical Systems, Oro Valley, AZ, USA). Tissues were again washed and then incubated with the primary antibody directed against Ki67 (Dako, clone: MIB-1; 1:150). Subsequently, tissues were incubated with polymer for 10 min and developed with DAB-Chromogen for 10 min. Experiments were repeated at least three times. IHC staining of MFF was performed on duplicate cores of 10 cases of MM and 11 normal bone marrow tissue (N) of a TMA slide (cat. BM483b; Biomax). TMA slide was processed by using the automated Dako Autostainer, with the EnVision™ FLEX

DAB+ Substrate Chromogen System DAB IHC Detection Kit (GV825 Dako Omnis, Denmark). To remove paraffin, the TMA slide was thawed at RT for 30 minutes, followed by incubation in a 65°C dry oven for 30 minutes. After dewaxing and hydration, antigen retrieval was performed by microwaving the samples in sodium citrate buffer (pH 8.0) for 20 min. The slide was then treated with a peroxidase blocker for 10 minutes, followed by closure in 5% BSA solution for 30 min. TMA slide was subsequently incubated with MFF primary antibody, followed by a secondary antibody incubation. Finally, DAB chromogenic solution was added, and the slide was counterstained with hematoxylin and mounted with cover glass.

### Statistical analysis

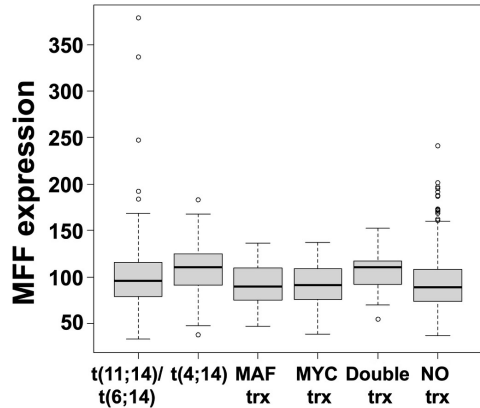
Each *in vitro* experiment was performed at least three times and values are reported as mean  $\pm$  SD. Comparison between groups was determined by Student's t-test, while statistical significance of differences among multiple groups was determined by GraphPad software ([www.graphpad.com](http://www.graphpad.com)). A *p*-value < 0.05 was accepted as statistically significant. Graphs were obtained using Graphpad Prism version 8.0 (GraphPad Software, La Jolla, CA, USA).

### Supplementary references

1. Morelli E, Hunter ZR, Fulciniti M, et al. Therapeutic activation of G protein-coupled estrogen receptor 1 in Waldenström Macroglobulinemia. *Exp Hematol Oncol* 2022;11(1):54.
2. Becherini P, Soncini D, Ravera S, et al. CD38-Induced Metabolic Dysfunction Primes Multiple Myeloma Cells for NAD<sup>+</sup>-Lowering Agents. *Antioxidants* 2023;12(2):494.
3. Miller C, Yesil J, Derome M, et al. A Comparison of Clinical FISH and Sequencing Based FISH Estimates in Multiple Myeloma: An MmrF Compass Analysis. *Blood* 2016;128(22):374–374.
4. Todoerti K, Ronchetti D, Favasuli V, et al. DIS3 mutations in multiple myeloma impact the transcriptional signature and clinical outcome. *Haematologica* 2021;107(4):921–932.
5. Zhang B, Wang Q, Lin Z, et al. A novel glycolysis-related gene signature for predicting the prognosis of multiple myeloma. *Front Cell Dev Biol*;11.
6. Torcasio R, Gallo Cantafio ME, Veneziano C, et al. Targeting of mitochondrial fission through natural flavanones elicits anti-myeloma activity. *J Transl Med* 2024;22(1):208.
7. Gallo Cantafio ME, Torcasio R, Scionti F, et al. GPER1 Activation Exerts Anti-Tumor Activity in Multiple Myeloma. *Cells* 2023;12(18):2226.
8. Amodio N, Gallo Cantafio ME, Botta C, et al. Replacement of miR-155 Elicits Tumor Suppressive Activity and Antagonizes Bortezomib Resistance in Multiple Myeloma. *Cancers (Basel)* 2019;11(2):236.
9. Chou T-C. Drug Combination Studies and Their Synergy Quantification Using the Chou-Talalay Method. *Cancer Res* 2010;70(2):440–446.

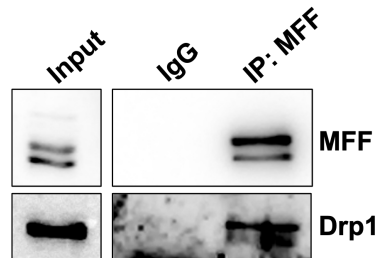
# Supplementary Figure 1

**A**

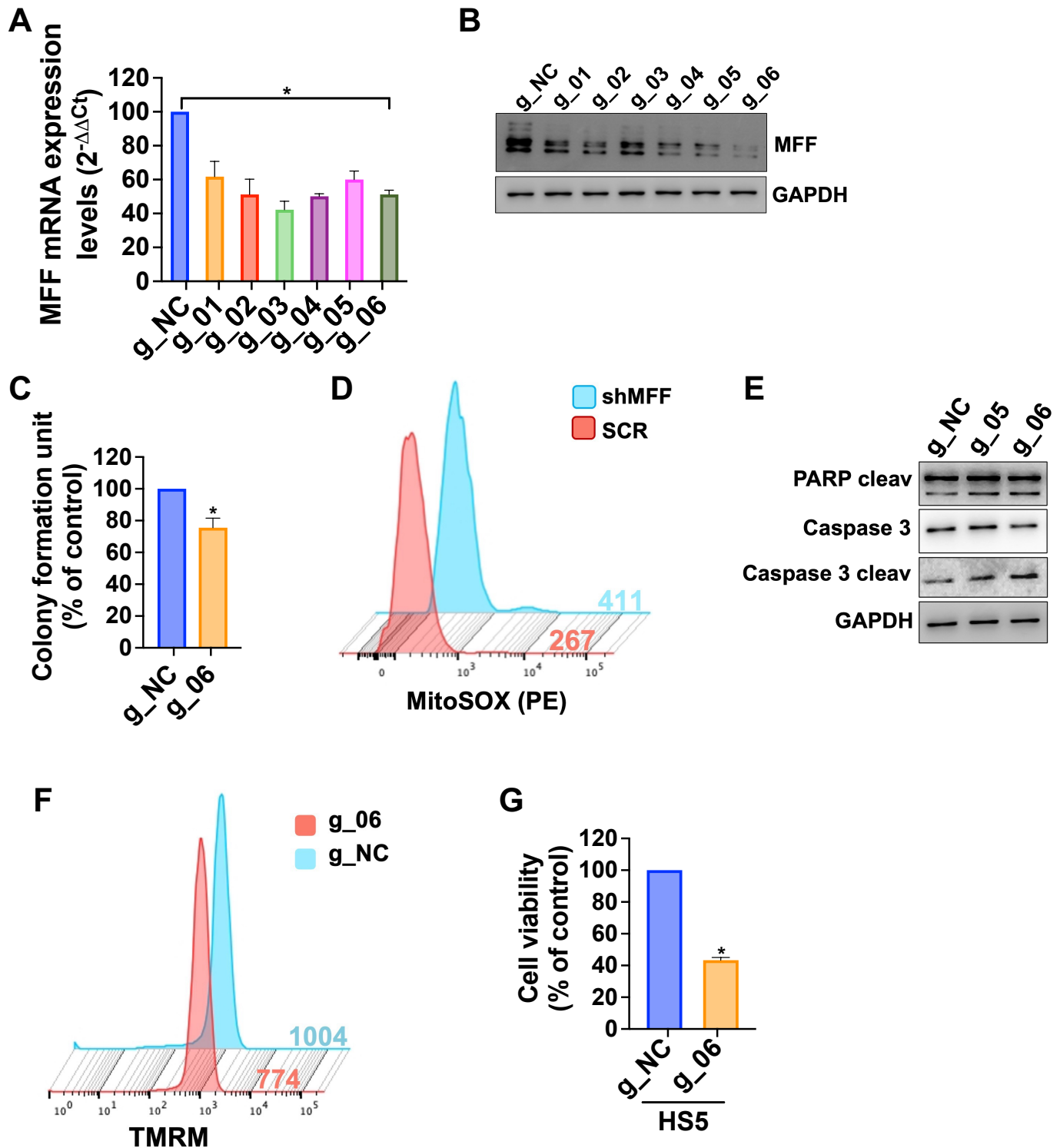


	t(11;14)/ t(6;14)	t(4;14)	MAF trx	MYC trx	double trx
t(4;14)	<b>0.0007</b>				
MAF trx	0.108	<b>0.0004</b>			
MYC trx	0.189	<b>0.0042</b>	0.470		
double trx	0.081	0.423	<b>0.023</b>	<b>0.041</b>	
NO trx	<b>0.0086</b>	<b>0.00001</b>	0.479	0.449	<b>0.0100</b>

**B**

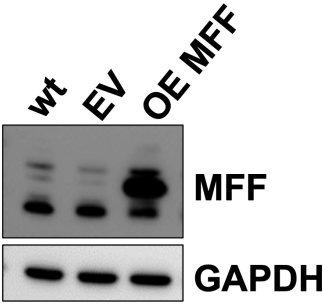


# Supplementary Figure 2

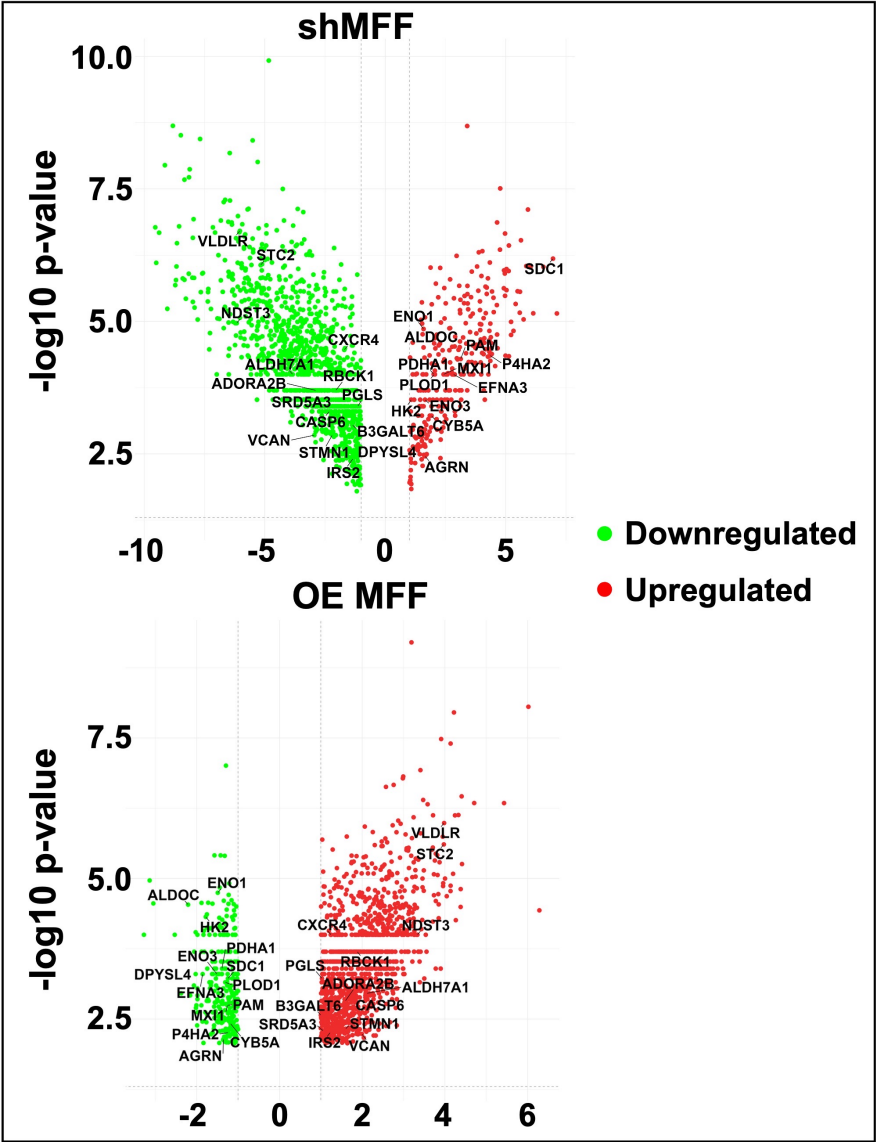


Supplementary Figure 3

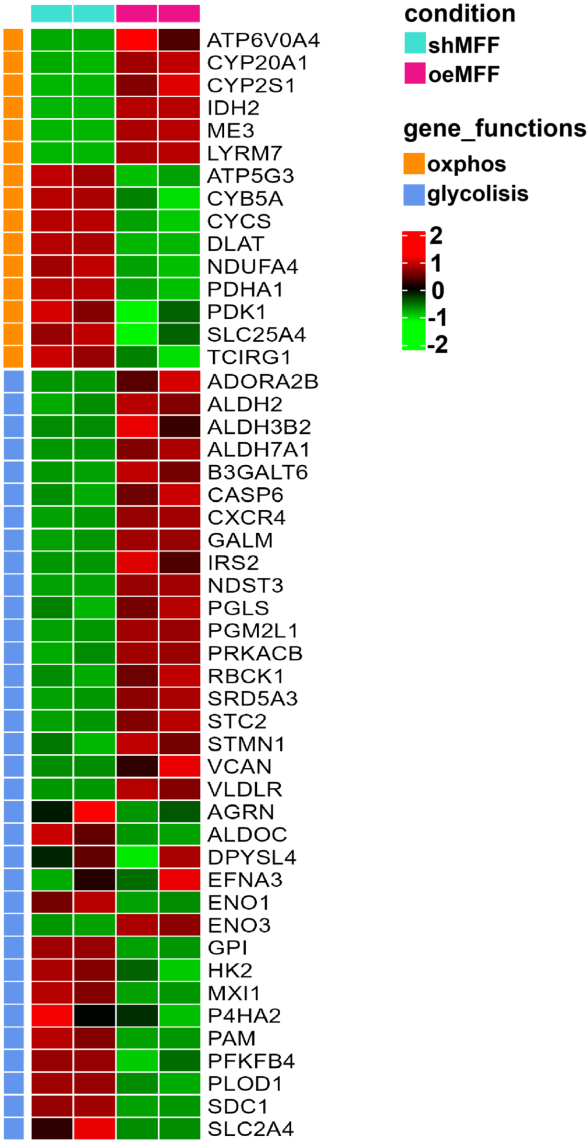
A



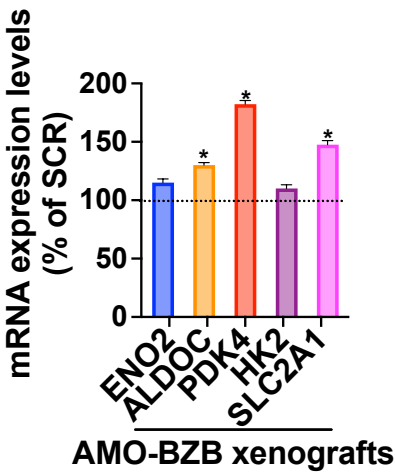
B



C

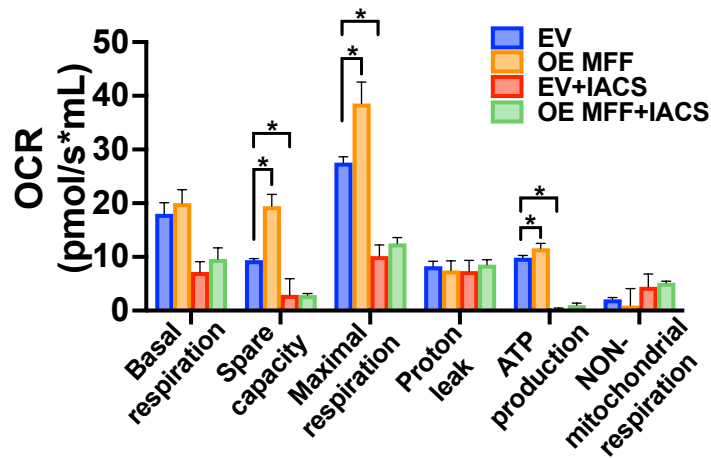


D

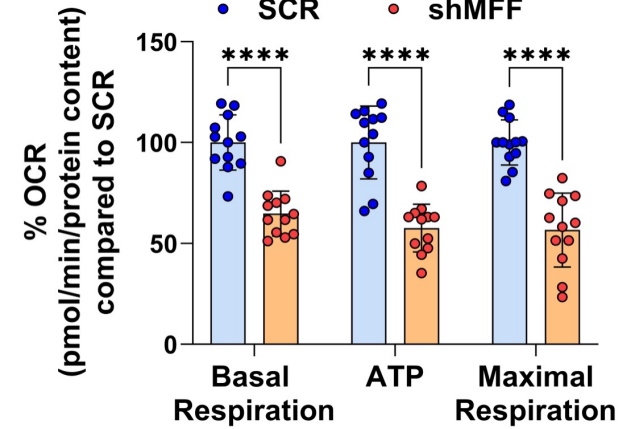
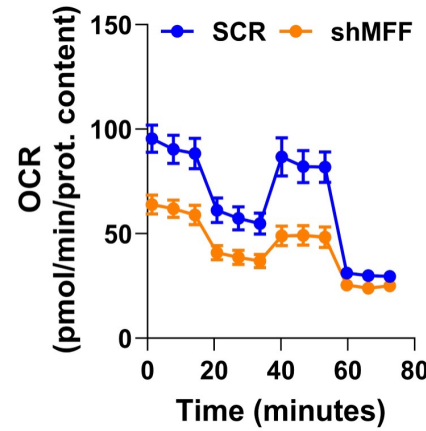


# Supplementary Figure 4

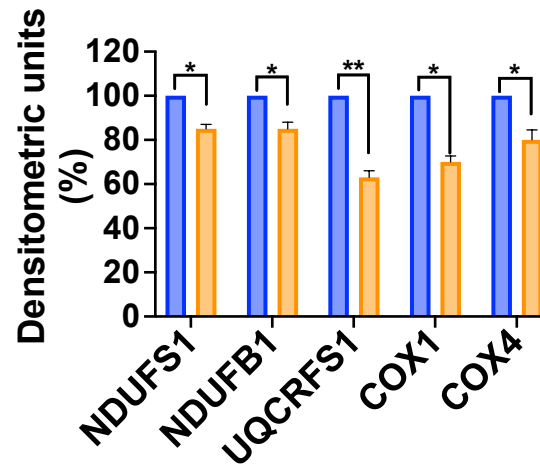
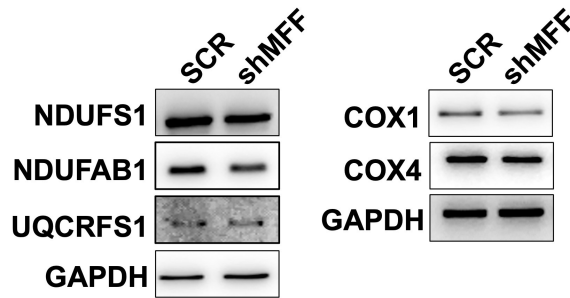
**A**



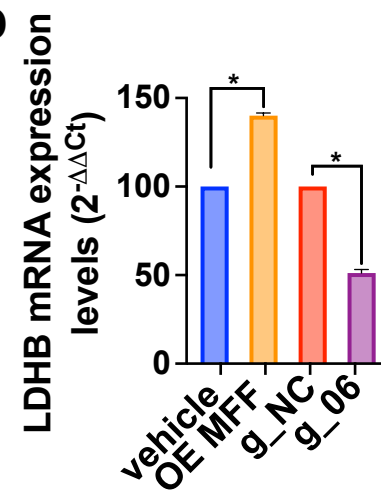
**B**



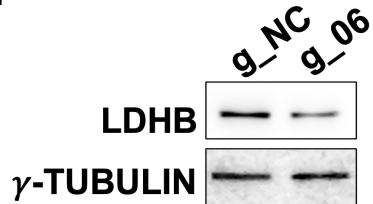
**C**



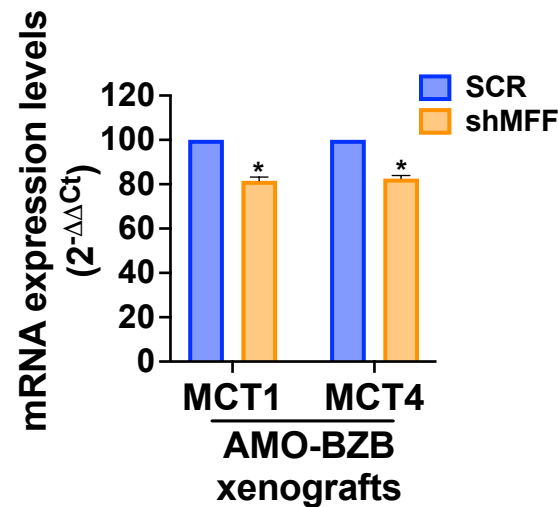
**D**



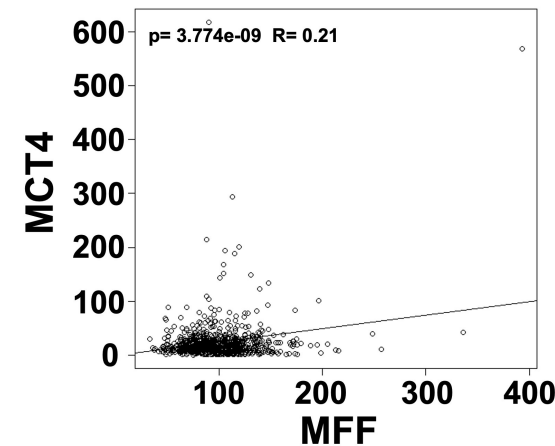
**E**



**F**



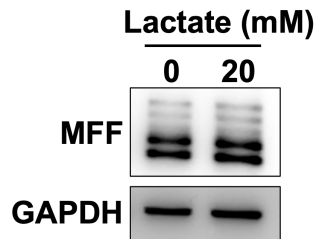
**G**



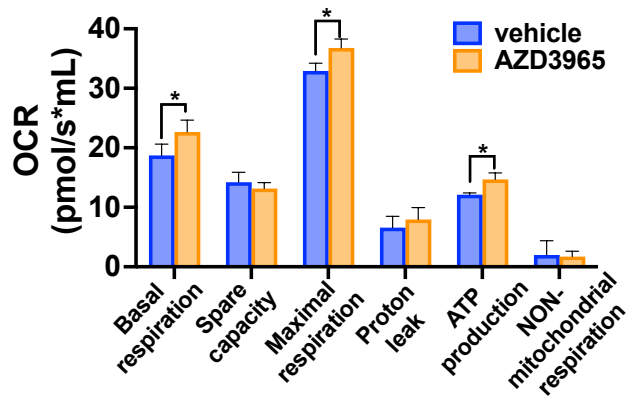


# Supplementary Figure 5

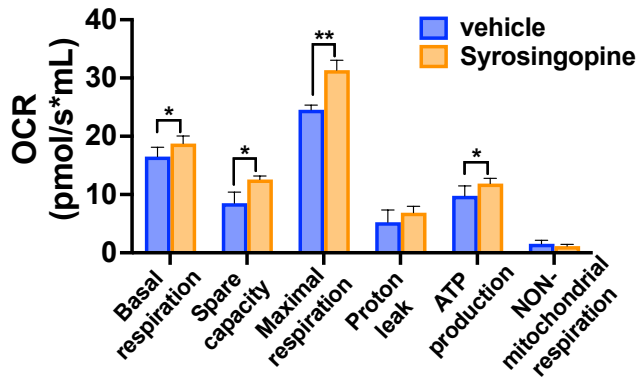
**A**



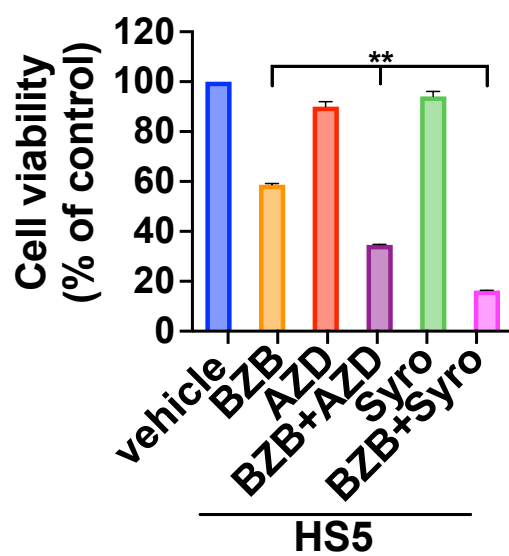
**B**



**C**



## Supplementary Figure 6



## Supplementary Figure Legends

**Supplementary Figure 1. A)** Box plot of MFF expression in 774 cases of the CoMMpass cohort stratified according to the main IgH translocations, including: t(11;14)/t(6;14) (n=162); t(4;14) (n=99); MAF translocated (trx) (n=43); MYC trx (n=24); double trx (n=17), and non-trx (n=429) MM patients. Kruskal-Wallis test was applied to assess differences in expression levels between groups. The significant pairwise comparisons are performed by the Dunn test.  $p = 5.762 \times 10^{-7}$ . **B)** Western blot analysis of Drp1 and MFF proteins in whole-cell lysates (input) and anti-MFF immunoprecipitation products obtained from AMO-BZB cells.

**Supplementary Figure 2. A)** Quantitative RT-PCR analysis of MFF mRNA expression levels in AMO-BZB cells, 48h after electroporation with gapmeRs g\_01, g\_02, g\_03, g\_04, g\_05, g\_06, or g\_NC (control). The results show the average  $\pm$  standard deviation (SD) of mRNA expression levels after normalization with GAPDH and  $\Delta\Delta C_t$  calculations.  $*p < 0.05$ . **B)** Western blot analysis of MFF expression in AMO-BZB cells, 48h after electroporation with gapmeRs g\_01, g\_02, g\_03, g\_04, g\_05, g\_06, or g\_NC (control). GAPDH was used as loading control. **C)** Colony formation assay was performed on AMO-BZB cell line after electroporation with g\_06 and g\_NC, and seeded on methylcellulose for 10 days. Histogram bars reported the mean  $\pm$  SD of three independent experiments.  $*p < 0.05$ . **D)** Flow cytometry analysis of mitochondrial ROS levels after staining of AMO-BZB cells with MitoSOX Red probe. Histogram is representative of three independent experiments. Mean fluorescence intensity (MFI) values are reported. **E)** Western blot analysis of PARP and Caspase 3 in AMO-BZB cells, 48h after electroporation with g\_06 or g\_NC; GAPDH was used as loading control. **F)** Flow cytometry analysis of mitochondrial membrane potential after staining of AMO-BZB cells with TMRM probe, 48h after electroporation with g\_06 or g\_NC. Histogram is representative of three independent experiments; mean fluorescence intensity (MFI) values are reported. **G)** Cell viability assessed by Cell Titer Glo assay in AMO-BZB cells electroporated with g\_06 or g\_NC, and then co-cultured with HS5 cells for 48h. Cell viability was expressed as the percentage of g\_NC. Data represent the average  $\pm$  SD of three independent experiments.  $*p < 0.05$ .

**Supplementary Figure 3. A)** Western blot analysis of MFF expression in H929 after lentiviral expression of MFF cDNA (OE MFF) or the corresponding empty vector (EV); GAPDH was used as loading control. **B)** Volcano plot representation of differential expression analysis of genes in shMFF AMO-BZB and OE MFF H929 MM cells. The x-axis indicates the expression fold change (log2) and the y-axis indicates the p-value ( $-\log_{10}$ ) for each gene versus control; the fold change threshold considered was greater than 2 or less than -2.  $p < 0.05$ . Upregulated (red) and downregulated (green) transcripts are shown; selected representative genes are labeled. **C)** Heatmap shows genes related to glycolysis or oxidative phosphorylation pathways, with opposite expression trend between shMFF AMO-BZB and OE MFF H929 cells. **D)** Quantitative RT-PCR analysis of ALDOA, ENO2, HK2, PDK4, and SLC2A1 mRNA expression levels in AMO-BZB xenografts retrieved from mice. The results show the average of mRNA expression levels after normalization with  $\beta$ -Actin and  $\Delta\Delta C_t$  calculations and are expressed as percentage  $\pm$  standard deviation (SD) normalized to the respective control for each condition.  $*p < 0.05$ .

**Supplementary Figure 4. A)** Real time oxygen consumption rate (OCR) measurement, 24h after treatment of OE MFF H929 cells with IACS-010759 (250 nM). Histogram bars report the average of three independent experiments performed through OROBOROS instruments.  $*p < 0.05$ . **B)** Seahorse analysis of OCR measurement on shMFF AMO-BZB MM cells; at least six replicates were performed in each experiment. Results are the average of three independent experiments and are expressed as percentages normalized to the control  $\pm$  standard error of mean (SEM).  $****p < 0.001$ . **C)** Western blot analysis of NDUFS1, NDUFB1, UQCRC1, COX1, and COX4 protein expression in AMO-BZB cells after lentiviral shMFF transduction. GAPDH was used as loading control. Histogram bars represent the densitometric analysis, reported as fold increase relative to the vehicle control.  $*p < 0.05$ ;  $**p < 0.01$ . **D)** Quantitative RT-PCR analysis of LDHB mRNA expression levels in OE MFF H929 cells and in AMO-BZB cells after electroporation with g\_06 or g\_NC. The results show the average of mRNA expression levels after normalization with  $\beta$ -Actin and  $\Delta\Delta C_t$  calculations, and are expressed as percentage  $\pm$  standard deviation (SD) normalized to the respective control for each condition.  $*p < 0.05$ . **E)** Western blot analysis of LDHB expression in AMO-BZB cells, 48h after electroporation with g\_06 or g\_NC;  $\gamma$ -tubulin was used as loading control. **F)** Quantitative RT-PCR analysis of MCT1 and MCT4 mRNA expression levels in AMO-BZB xenografts. The results show the average  $\pm$  SD of mRNA expression levels after normalization with  $\beta$ -actin and  $\Delta\Delta C_t$  calculations.  $*p < 0.05$ . **G)** Pearson's correlation analysis of MFF and MCT4 gene expression in the CoMMpass global dataset including 774 MM cases; linear regression is shown as a dotted line.

**Supplementary Figure 5. A)** Western blot analysis of MFF expression in AMO-BZB cells, 48h after treatment with Lactate; GAPDH was used as loading control. Real time oxygen consumption rate (OCR) measurement, 24h after treatment with **(B)** AZD3965 (25  $\mu$ M) or **(C)** Syrosingopine (2.5  $\mu$ M) in AMO cells;

histogram bars report the average of three independent experiments performed through OROBOROS instrument. \* $p < 0.05$ ; \*\* $p < 0.01$ .

**Supplementary Figure 6.** Cell Titer Glo assay of AMO cells treated with Bortezomib (1.5 nM) alone or in combination with Syrosingopine (2.5  $\mu\text{M}$ ) or AZD3965 (25  $\mu\text{M}$ ), and co-cultured with HS5 cell lines for 48h. Cell viability was expressed as the percentage of vehicle-treated cells. Data represents the average  $\pm$  standard deviation (SD) of three independent experiments. \*\* $p < 0.01$ .